ERJ
Engineering Research Journal
Faculty of Engineering
Menoufia University

TRANSIENT AND STEADY STATE PERFORMANCE CHARACTERISTICS OF A THERMOELECTRIC GENERATOR

Ahmed S. El-Adl[1], M.G. Mousa[2], E.A. Abdel-Hadi[3] and A.A. Hegazi[2]

[1] *Department of Mechanical Engineering, Higher Technological Institute, Tenth of Ramadan City, Egypt*
[2] *Department of Mechanical Power Engineering, Mansoura University, Mansoura, Egypt.*
[3] *Department of Mechanical Power Engineering, Benha University, Shoubra, Egypt.*
[1]***Tel**: +02 0124566764*
[1]***Email Address**: ahmed.s.eladl@hti.edu.eg*

ABSTRACT

The global energy and environmental issues are promoting the development of innovative energy solutions. Thermoelectric generators (TEGs) are regarded as a promising alternative to conventional energy technologies. TEG is a device that converts thermal energy directly into electric power by exploiting Seebeck effect. It is essential to understand the behavior of thermoelectric devices during both thermal transient and steady state to accurately simulate and design complex and dynamic thermoelectric systems. So a comprehensive model for simulating the dynamic TEG performance is developed, taking into consideration all the thermoelectric effects (Seebeck, Peltier and Thomson), in addition to Joule heating and Fourier heat conduction. Additionally, the effects of temperature-dependence of thermoelectric materials are accounted. Computational results are retrieved using "MATLAB" software. To verify the integrity of the modeling processes, the predicted results are compared with data obtained from the experimental evaluation. It is found that the outcomes of the experimental analysis validated the accuracy of the developed model and the possibility to be used as a simulation tool. The dynamic performance characteristics of a TEG is experimentally studied under different operating conditions. The effect of input heat rate and the influence of utilizing extended surfaces (fins) on both transient and steady state performance of a TEG are experimentally investigated. The variation in the temperature of the TEG hot and cold sides in addition to the output voltage is taken as a denotation of the performance characteristics. Input heat rate of 15.0 W, 17.5 W, 20.0 W, 22.0W and 25.0 W are applied to the TEG hot side. Free air convection is the utilized for heat dissipation from the TEG module through the cold side. From the experimentation, it can be deduced that increasing the input heat rate provides higher temperature difference across the module sides leading to higher power output. Additionally, using fins to aid heat dissipations enhanced the TEG performance by lowering the temperature of cold side and increasing the temperature difference across the module. The experimental data obtained are compared with the data available by the TEG module manufacturer and excellent agreement is obtained.

الملخص :

المولدات الكهرحرارية هي واحدة من موارد الطاقة الجديدة، النظيفة، الواعدة والفعالة من حيث الأداء والتكلفة. وتلك المولدات عبارة عن أجهزة صلبة مكونة من مواد شبه موصله تحول الطاقة الحرارية مباشرة إلى طاقة كهربائية بكمية تعتمد على الفرق في درجة الحرارة المؤثر عليها. أن أداء المولدات الكهرحرارية يخضع لتأثيرات حرارية وكهربائية مختلفة تبعاً لظروف التشغيل، ولذلك يتم في هذا البحث تطوير نموذج شامل لمحاكة أداء مولد كهر حراري اثناء التشغيل سواء في الحالة الديناميكية أو المنتظمة. خلال النموذج يؤخذ في الاعتبار جميع التأثيرات الكهرحرارية (سيبيك، بلتيير وطومسون)، بالإضافة إلى تأثير جول والتوصيل الحراري مع الاخذ بالاعتبار اعتماد خواص المواد الكهرحرارية على درجة الحرارة. ووجد ان نتائج المحاكاة تتوافق بشكل جيد مع القياسات التجريبية الخاصة بالدراسة الحالية، كما انها تتوافق جيداً ايضاً مع نتائج المحاكاة للنماذج الاخرى الموجودة بالأبحاث. تجريبياً تم إجراء اختبارات على مولد كهرحراري لدراسة تأثير معدل الطاقة الحرارية المدخلة للمولد من خلال الجانب الساخن بالإضافة الى تأثير تبريد الجانب البارد باستخدام الأسطح الممتدة (الزعانف). وفقا للنتائج التجريبية، يتضح أن زيادة معدل الطاقة الحرارية المدخلة من خلال الجانب الساخن للمولد يعزز من الأداء وأيضاً استخدام الزعانف يحسن من أداء المولد عن طريق خفض درجة حرارة الجانب البارد وبالتالي زيادة من فرق درجة الحرارة بين الجانبين. بمقارنةً النتائج التجريبية بالبيانات المقدمة من قبل الشركة المصنعة للمولد ووجد تقارباً مرضياً بين النتائج.

***Keywords*:** Thermoelectric generator (TEG), power output, conversion efficiency, transient and steady state performance.

Nomenclature

A	Cross-section area, (m^2)	*Greek symbols*	
Bi_2Te_3	Bismuth Telluride	β	Thomson coefficient, (V/K)
FC	Free convection	Δ	Difference
FEM	Finite element method	η	Efficiency, (%)
I	Electric current, (Amp.)	Ω	Ohm
k	Thermal Conductivity, (W/m K)	σ	Electric conductivity, (S)
L	length, (m)	*Subscript*	
n	Negative	c	Conversion
N	Number	cj	Cold junction
p	Positive	H	Electric heater
P	Power	hi	Hot junction
Q	Heat rate (W)	in	Input
R	Electric resistance,(W)	L	Load
S	Seebeck coefficient, (V/K)	n	n-type
T	Absolute temperature, (K)	O	Output
TEG	Thermoelectric generator	p	p-type
TIM	Thermal interface material	pn	Thermocouple
V	Voltage, (V)		
ZT	Figure of merit		

1. Introduction

The acceleratory asymmetry between demand and provision supply of energy and continual energy abjection motivates the researchers to inquire environmental affable, clean energy resources. Thermoelectric devices are among the most promoting and cost-efficient energy resources. TEG provides versatile advantages over conventional power generators. TEG offers various advantages over traditional power generators. TEGs are robust solid-state energy converters that have no mechanical moving parts and hence are silent, lightweight, reliable, durable, compact, maintenance-free, long operating periods, uncomplicated scalability and environmentally friendly. The use of TEGs has increased rapidly in recent years with applications ranging from microwatts to kilowatts. One of the most important application, is the recovery of waste heat from industrial processes [20], in addition to the recovery of automotive waste heat [16]. Also, TEGs can be used to produce electricity by direct conversion of renewable energy such as solar energy [17]. Moreover, due to their robustness, thermoelectric generators are suitable for specialized applications such as aerospace, medical, military and telecommunications. [5]. A typical TEG module consists of a number of semiconductor pairs. Each pair includes a "p-type" (hole carriers) and an "n-type" (electron carriers) thermoelements (i.e., pellet) connected through metallic electrical contact pads, this pair is known as a thermoelectric couple (or thermocouple) which is shown in figure 1. [6].

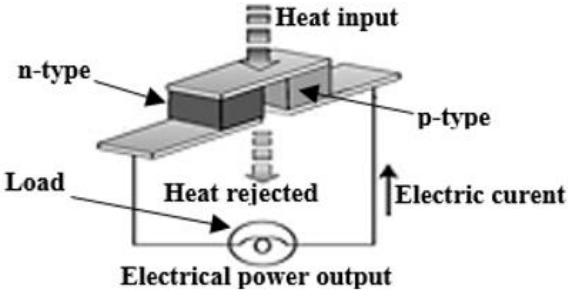

Figure 1. Schematic diagram of a single thermoelectric couple (Thermocouple) [1].

In the module, thermocouples are connected electrically in series with metal connecting strips and thermal in parallel, sandwiched between two electrically insulating and thermally conducting ceramic plates. A cut-away view of a typical TEG module is shown in figure 2.

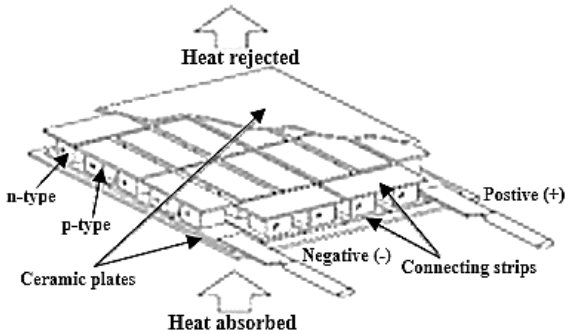

Figure 2. Cut-away view of a typical TEG module [1].

The efficiency of thermoelectric materials greatly depends on the figure of merit, $ZT = \frac{S^2\sigma}{k}T$, where "S" is the Seebeck coefficient, "σ" is the electric conductivity, "k" is the thermal conductivity, and "T" is the absolute temperature at which the properties are measured. [9]. Thermoelectric materials with high ZT values have been developed continuously [15 and 22]. In addition to exploring thermoelectric materials properties, optimizing the geometrical shape and design of thermoelectric module have been considered continuously [13 and 21]. Employing appropriate model to characterize the performance is very critical and gained numerous investigations. **Chen et al.** [14] and **Apertet et al.** [2] analytically developed a model to analyze the performance of a thermoelectric generator. The results showed that the model predicted the system power output with reasonable accuracy. Using an electric analogy, **Barry et al.** [11] introduced one-dimensional thermal resistance network coupled with a co-optimization algorithm that simultaneously optimized thermoelectric leg length and cross-sectional area to maximize thermal conversion efficiency and maximum power output. Numerically, **Shen et al.** [18] proposed one-dimensional steady analysis theoretical model for analyzing the performance of thermoelectric generators. Their results showed that the form of the developed model was very simple and when the temperature-dependence of thermoelectric materials was not properly taken into account, the performance of TEG may be overestimated or underestimated. Also, commercial software based on the finite element method (FEM) can model thermoelectric devices. **Admasu et al.** [4] conducted finite element modeling and analysis to compare the outputs of the thermoelectric power generation system, which had uniform temperature distribution with that without uniform temperature distribution over the heat spreader. Finite element based software (ANSYS Workbench) was employed to simulate the system. The simulation results showed that maintaining the temperature distribution uniform all over the top surface of the heat spreader of the thermoelectric generator delivers better outputs.

Considerable research studies were also experimentally carried out to examine thermoelectric power generation and device efficiency. **Sarhadi et al.** [12] presented the influence of using different interface materials on power-producing capabilities of a TEG as a function of flow rate. Three different thermal interface materials were assessed. The optimal thermal interface material was shown to be graphite paper.

The influence of metal foams on the performance of thermoelectric waste heat recovery system was experimentally investigated by **Wang et al.** [19]. The results showed that filling metal foams in the flow channels could efficiently enhance the performance of the TEG. A comparison between the thermal performances of thermoelectric generators with the cold sides cooled by either bare plate, 60 mm fin, 80 mm fin and 100 mm fin is presented by **Date et al.** [10]. It was concluded that the increasing the fin length from 60 mm to 100 mm did not have as much effect on the cooling capacity and similarly did not had as much effect on power generation capacity from the thermoelectric generators. **Montecucco et al.** [8] analyzed the impact of thermal imbalance on the power produced from arrays of thermoelectric generators connected in series and parallel. The presented results suggested that series electrical connection enabled more of the available power to be captured. Thermoelectric power enhancement of a liquid-to-liquid TEG was investigated by **Lesage et al.** [7]. Three different geometric forms of flow turbulating inserts were fitted into the channels of the thermoelectric generator. Spiral inserts were shown to offer a minimal improvement in thermoelectric power production whereas inserts with protruding panels are shown to be the most effective. **Rezania et al.** [3] studied the power generated versus the coolant pumping power in the TEG. The results showed that there is a unique coolant flow rate at any temperature difference that makes maximum net-power in the system.

Concluding from the literature, that there is a significant push to increase the output power of TEGs by enhancing their performance to make them more competitive energy technology. So in the present study, the influence of the different operating conditions on the transient and steady state performance characteristics of a TEG are theoretically and experimentally investigated. Operating aspects of the TEG system such as hot side temperature, cold side temperature, closed circuit voltage and power output are studied. A comprehensive theoretical model is developed to simulate and predict the performance of the TEG. Also, the effect of input heat rates through the TEG hot side in addition to utilizing fins to aid heat dissipation from the module cold side on the TEG performance is experimentally demonstrated.

2. Model description

The mathematical model is developed based on the law of conservation of energy, to analyze the performance of the TEG. Some assumptions are made to simplify the complex process of heat conversion and heat transfer taking place in the operation of the TEG without losing significant

accuracy. These assumptions include that all the p-type and n-type thermoelements are identical, homogenous and have the same geometrical parameters. In addition, the simulated module is well insulated electrically and thermally from the surrounding expect at the junction-reservoir contacts. So, one dimension heat transfer is considered. The analysis is presented for a single thermocouple, which can afterthought be extended to the remaining module couples by summing the power output of all thermocouples. The analyzed thermoelectric couple consists of a p-type and n-type doped semiconductor thermoelements. These elements are connected in series by copper conducting strips and sandwiched between two layers of thermal conducting and electrically insulating ceramic substrates. The ceramic substrates are covered by a layer of thermal interface material (TIM) to decrease the thermal resistance between the heat source, module and the heat sink, respectively. The couple operates between constant heat rate source and a heat sink at a constant temperature and the voltage produced by the couple is connected in a circuit to a load resistor. Referring to figure 3, energy balance for the system is set up to obtain the governing equations of the system that couples the thermal and electric effects. The energy balance method is based on subdividing the thermocouple into a sufficient number of volume elements and then an energy balance is applied on each element. The transient system of the governing equations are solved simultaneously using an explicit forward approximation in time to determine the temperature distribution along the module as a function of time. In transient problems, the superscript "i" is used counter of time steps, with "i = 0" corresponding to the specified initial condition.

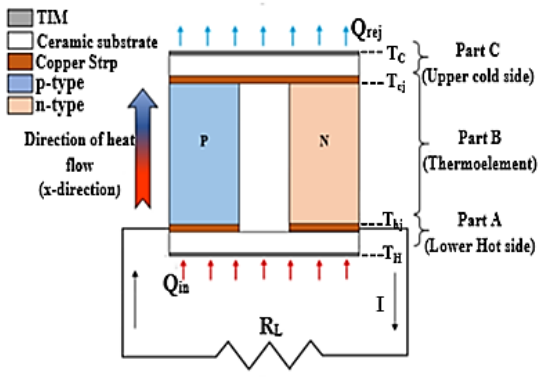

Figure 3. Schematic diagram of a thermocouple utilized for modeling.

The magnitudes of the heat input and output from hot and cold junctions respectively can, therefore, be written as [14 and 23]:

$$Q_{hj} = S^i_{pn|h} T^i_{hj} I^i - 0.5\, I^{i2} R^i_{pn|h} + k^i_{pn|h} A_{pn} \frac{(T^i_{hj} - T^i_{cj})}{L_{pn}} - 0.5 I^i \beta^i_{pn|h} (T^i_{hj} - T^i_{cj}) \quad \dots (1)$$

$$Q_{cj} = S^i_{pn|c} T^i_{cj} I^i + 0.5\, I^{i2} R^i_{pn|c} + k^i_{pn|c} A_{pn} \frac{(T^i_{hj} - T^i_{cj})}{L_{pn}} + 0.5 I^i \beta^i_{pn|c} (T^i_{hj} - T^i_{cj}) \quad \dots (2)$$

, where S^i_{pn} is Seebeck coefficient (V/K), R^i_{pn} is the internal module resistance (Ω), k^i_{pn} is the thermal conductivity of the thermocouple (W/m.K), "β^i_{pn}" is the Thomson coefficient (V/K), "A_{pn}", "T^i_h" and "T^i_c" are cross-sectional area of the thermoelement (m^2), the temperature of hot and cold junctions (°C), respectively. The first term in Eq. (1) and Eq. (2) is for Peltier heat, the second term stands for Joule's heat, the third term represents the Fourier's heat conduction and the fourth term refers to the Thomson heat. The elements have uniform cross section area "A_{pn}" (m^2) and are equal in length "L_{pn}" (m).

The Thomson coefficient "β", can be expressed by the Kelvin relation, where the Thomson coefficient is related to the Seebeck coefficient as follow [23]:

$$\beta^i_{pn} = T^i \frac{dS^i_{pn}}{dT} \quad \dots (3)$$

The module thermal conductance is given by [14]:

$$k^i_{pn} = k^i_p + k^i_n \quad \dots (4)$$

, and, the electrical resistance of the module is given by [14]:

$$R_{pn} = R^i_p + R^i_n = \frac{L_p}{\sigma^i_p A_p} + \frac{L_n}{\sigma^i_n A_n} = \frac{L_{pn}}{A_{pn}} \left(\frac{1}{\sigma^i_p} + \frac{1}{\sigma^i_n} \right) \quad \dots (5)$$

, where "R^i_n", "R^i_p", "σ^i_p" and "σ^i_n" are the resistance and electric conductance of n-type, p-type semiconductors thermoelements, respectively. The current through the module at the matched load, which is the same for all the thermocouple due to series connection, is given by [9]:

$$I^i = \frac{S^i_{pn} (T^i_h - T^i_c)}{R^i_{pn} + R_L} \quad \dots (6)$$

, where "R_L" is the resistance of the load. Then, the module output voltage proportional to the temperature difference and at the matched load across the TEG module is given by:

$$V^i = I^i \times R_L \quad \dots (7)$$

Therefore, for "N_{pn}" thermocouples, the total power output produced by the module at the matched load is given by:

$$P_o^i = N_{pn} \times V^i \times I^i \quad \dots (8)$$

For thermoelectric power generation, the conversion efficiency for the TEG module is defined as the ratio of the electric output power "P_o" delivered to a load of resistance "R_L", divided by the heat flow rate into the hot side of the TEG module, "Q_{in}", and is given by:

$$\eta^i = \frac{P_o^i}{Q_{in}} \quad \dots (9)$$

In this model, the thermoelectric couple is made of "Bismuth Telluride" (Bi_2Te_3). The TE properties as a function of temperature for both of p-type and n-type thermoelements are calculated by using formulas provided by European thermodynamic, Inc. [24].

3. Experimental Setup

The experimental setup is designed and constructed to study the performance characteristics of the TEG for both transient and steady states is shown in figure 4. A thermoelectric Bismuth Telluride (Bi_2Te_3) device designed for electric power generation, with a physical size of 62 mm × 62mm × 4.0 mm, containing 127 p-n couples connected in series has been used in this study. To provide the necessary thermal input to the device, the hot side was attached to a copper plate, heated with a nominal power of 277 W. The rate of heat input is adjusted using an electrical autotransformer (VARIAC) which connected to a voltage stabilizer to ensure constant input heat rate to the TEG. An assembly is created to house the TEG for the testing purposes. The assembly consists of two copper plates; one is placed between the heater and the hot side of the module, while the other plate is placed between the heat sink and the cold side. These copper plates are chosen for construction due to its high thermal conductivity. So, heat is distributed well and thus temperature measurements of both sides more convenient. The copper plates are insulated by Phenolic Laminated sheets (for electric and thermal insulation), where groves are made in these sheets to occupy the copper plates. The lateral area of the test section is heavily insulated with a thick layer of glass wool (excluded from figure 3) to prevent the heat loss from the test section to the surrounding. To ensure a proper thermal contact and minimum contact resistance, optimum-clamping force is applied on the TEG using screws and nuts. Additionally, a layer of thermal interface material is applied between the copper plates and both sides of the TEG along with optimal clamping force. Both hot and cold sides temperatures are measured using ten Chromel (Nickel-Chromium Alloy) / Alumel (Nickel-Aluminum Alloy) thermocouples (type K) with 0.2 mm wire diameter, where five thermocouples are used for each side. The two terminals of the TEG are connected with a non-inductive power resistor (0.47Ω) to form an electric circuit from which the output voltage and power output could be accurately measured. The side's temperature in addition to the output voltage is recorded using a data acquisition system, which is manufactured by National Instruments Co. Also, all the thermocouples are connected to temperature recorder through a multi-switch arrangement. The uncertainty in temperature measurements was ± 1.5°C. The utilized fins consist of 15 fins with 2 mm thickness and 16 mm height. The gap between the fins is 2 mm. Also, a layer of thermal interface material is placed between the fins and the upper surface of the cold side copper plate to ensure good contact between them. The fin is clamped over the copper plate through the usage of a pin – screw fixture threaded through two holes machined in the upper Phenolic Laminated sheet.

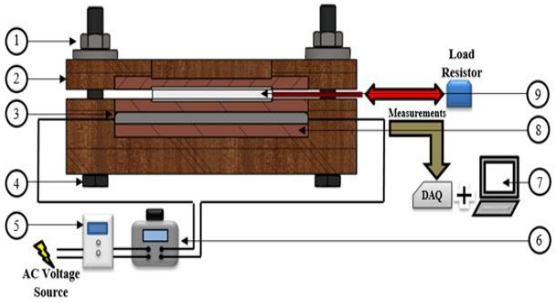

1. Nut, **2.** Phenolic Laminated sheet, **3.** Electric heater, **4.** Screw **5.** Voltage stabilizer, **6.** Autotransformer (VARIAC), **7.** Data acquisition system, **8.** Copper plate, **9.** TEG module.

Figure 4. Schematic diagram of the experimental setup.

4. Data Reduction

The experimental data obtained from the hot side temperature, cold side temperature, and output voltage are used to calculate the power output and conversion efficiency. At steady state condition, the produced heat generated by the electrical heating is given by the equation:

$$Q_{in} = \left(\frac{V_H^2}{R_H}\right) \quad \dots (10)$$

, where "Q_{in}" is the heat generation rate supplied by electric heaters (W), "V_H" is the applied voltage across the electric heater terminals (Volt) and R_h is the heater resistance (Ω).

The power output from the TEG can be derived from the following equation:

$$P_o = \left(\frac{V_o^2}{R_L}\right) \quad \dots (11)$$

, where "Po" is the power output (mW), "V_o" is the output voltage (mV) and "R_L" is the load resistor (Ω).

By measuring the power output of the TEG through a load, the conversion efficiency can be calculated as follow:

$$\eta_c = \frac{P_o}{Q_{in} \times 10^3} \quad \ldots (12)$$

, where "η_c" is the conversion efficiency (%).

5. Result and Discussion

In this section, the obtained theoretical and experimental results are interpreted and discussed to obtain a compressive view on the performance characteristic of the TEG. Additionally, the obtained predicted data from the simulation is compared with the data obtained from experimental work.

5.1 Simulation results

Transient simulation is used to predict different performance characteristics as a function of time. Figure 5 shows the predicted variation in the temperature of TEG both sides with time. Figures 5a and 5b illustrate the predicted variation in the temperatures of the hot side and the cold side with time, for input heat rates of 15W and 25W respectively.

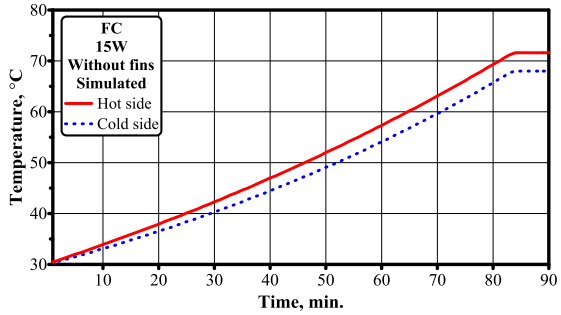

Figure 5a. Predicted variation in the temperature of both sides with time, for 15.0W input heat rate.

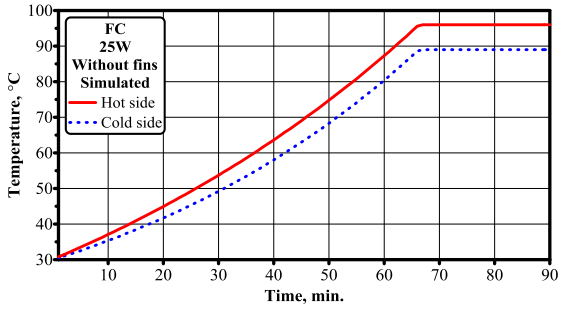

Figure 5b. Predicted variation in the temperature of both sides with time for 25.0W input heat rate.

Figure 5. Predicted variation in the temperature of both sides with time.

These figures indicate that the temperature of both TEG sides of the increases simultaneously with time until steady state operation is attained.

Figure 6 illustrates the predicted variation in the output voltage and corresponding power output of the TEG with time. From this figure, it can be concluded that the TEG output voltage follows the same trend of temperature, where the output voltage and subsequently power output increases simultaneously with increasing both sides temperature with time and until steady state operation is achieved. This can be attributed to the increase in the temperature difference between both sides, which in turn increases the output voltage and the corresponding power output.

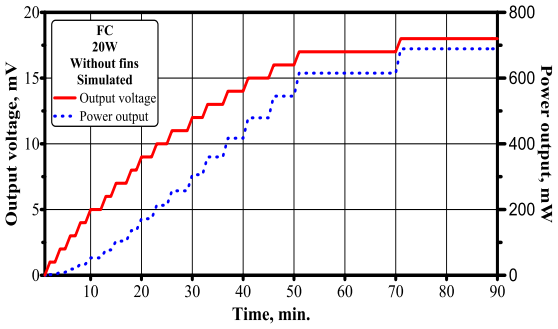

Figure 6. Predicted variation in output voltage and corresponding power output with time.

For comparison, the input heat rates used for simulation are similar to that used in experimental work. The effect of input heat rate on the predicted variation in the temperature of both sides with time is illustrated in figure 7. Figures 7a and 7b show the predicted variation in the temperatures with time for the hot and cold sides with various values of input heat rate, respectively. These figures indicate that the predicted variation in the temperature of TEG both sides is directly proportional to the rate of input heat.

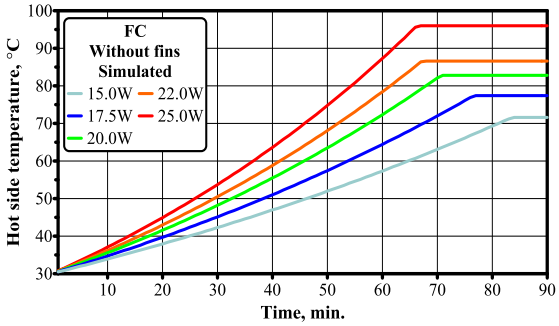

Figure 7a. Predicted variation in the hot side temperature with time for various input heat rates.

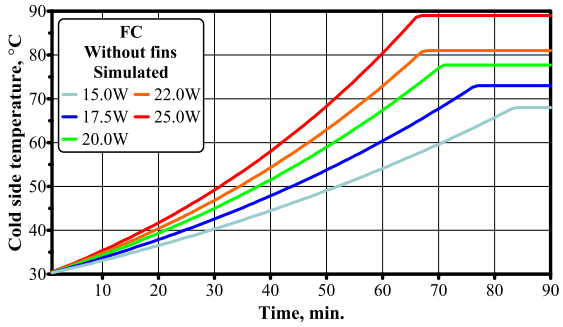

Figure 7b. Predicted variation in the cold side temperature with time for various input heat rates.

Figure 7. Predicted effect of input heat rate on the variation in the temperature of both sides with time.

Noting that the temperature of both sides follows the same trend, mainly due to the input heat conduction through the module from the hot side to the cold side, in addition to the other thermoelectric effects occurring inside the module.

The effect of input heat rate on the predicted variation in the TEG output voltage and corresponding power output with time is shown in figure 8.

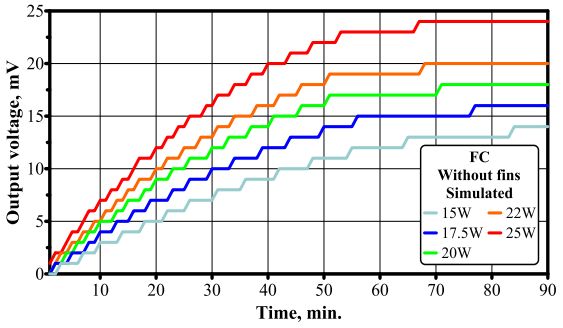

Figure 8a: Predicted variation in the output voltage with time for various input heat rates.

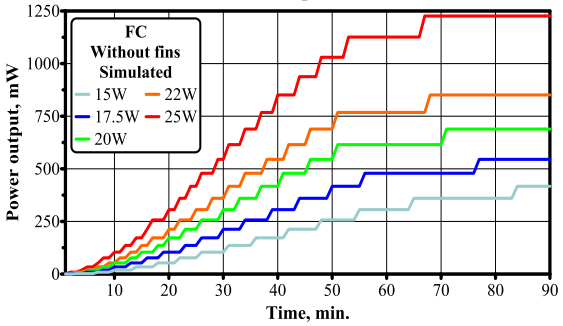

Figure 8b. Predicted variation in the power output with time for various input heat rates.

Figure 8. Predicted effect of input heat rate on the variation of the output voltage and the corresponding power output with time.

5.2 Experimental results

In experimental results, the effect of different operating conditions on both transient and steady state performance of the TEG module is presented. These figures illustrate that the output voltage and power output are also directly proportional to the value of heat input rate, as higher input heat rate will result in higher temperature difference across the TEG sides and subsequently higher output voltage

A comparison between the present experimental data of the variation in the power output with hot side temperature and those reported by the manufacturer [24] in case of FC assisted by a fin as a heat dissipation technique is illustrated in figure 9. An excellent agreement can be observed between both results, concluding that the power output increases almost linearly with increasing the hot side temperature. The coincident between the obtained experimental data and those from the manufacturer indicates the validity of the experimentation procedures applied and the accuracy of measurement. The slight discrepancies (i.e. within 2.5%) both results can be attributed to the difference between the used measurement techniques in the present study and that of used by the manufacturer.

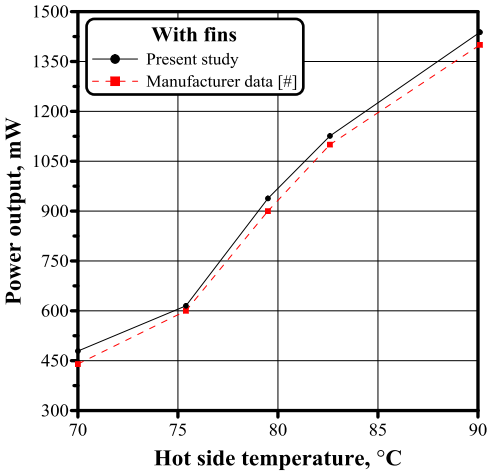

Figure 9. Comparison between the present experimental results and that after reference [24], for the variation in the power output with hot side temperature.

The effect of input heat rate on the variation of both sides temperature with time in case of FC is illustrated in figure 10. Figure 10a and 10b show the variation of the temperatures with time for the hot side and cold sides without and with fins for various values of input heat rate, respectively.

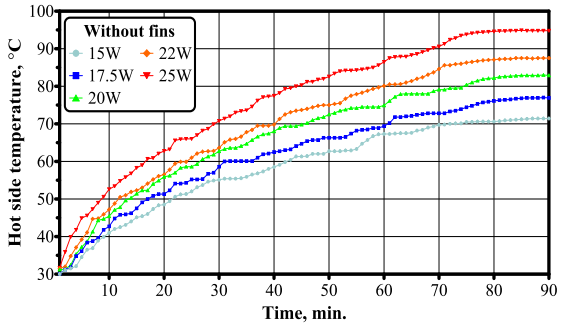

Figure 10a. Variation in the hot side temperature with time for various input heat rates, in case of FC without the aid of fins.

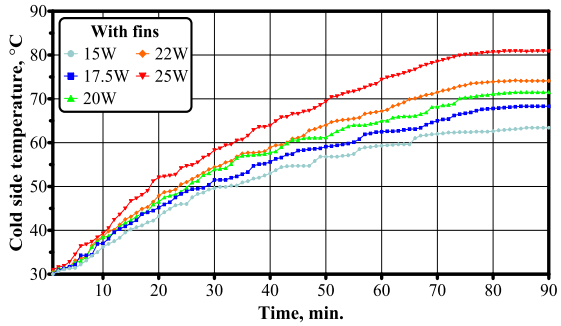

Figure 10b. Variation in the cold side temperature with time for various input heat rates, in case of FC with the aid of fins.

Figure 10. Effect of input heat rate on the variation in the temperature of both sides with time, in case of FC.

From these preceding figures, it can be concluded that for all the operating conditions in the experimental studies, the temperature of both sides increases with increasing the input heat rate, whereas the system heats up relatively quickly in the beginning and then slowly converts to steady state operation. Additionally, by comparing the temperatures of both sides for all operating conditions studied, it can be deduced that the temperature of the cold side is always lower than that of the hot side. This is related to the cooling effect provided by heat dissipation. In addition, it can be noticed that the temperature of both sides follows the same trend of transitory increase with operating time and until steady state is achieved. This occurrence is caused by the direct effect of heat conduction through the module from the hot side to the cold side. So the thermal conductivity of an excellent thermoelectric material should be relatively low so that a temperature difference can be established and maintained across the module. It is worthy to note that in addition to the effect of heat conduction (i.e., Fourier's heat), the temperature of both sides is also affected by Peltier effect, Joule heating and Thomson effect, which occur when a current flows through the module due to the connection of a load to the TEG output terminals.

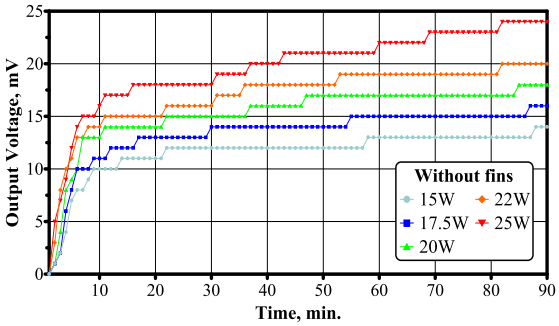

Figure 11a. Variation in the output voltage with time for various input heat rates in case of FC without the aid of fins.

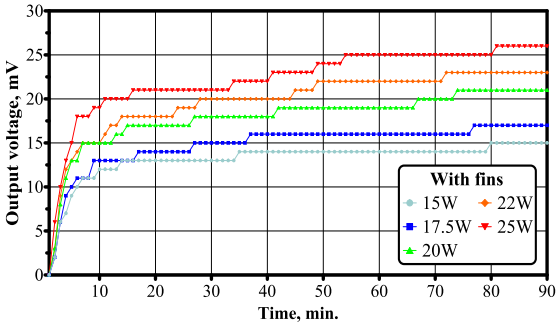

Figure 11b. Variation in the voltage output with time for various input heat rates in case of FC with the aid of fins.

Figure 11. Effect of input heat rate on the variation in the output voltage with time in case of FC.

The effect of input heat rate on the variation in the output voltage with time, in case of FC, is shown in figure 11. Figures 11a-11b demonstrate the variation of output voltage with time, in case of FC without and with the aid of fins, respectively for various values of input heat rate.

According to Seebeck effect, TEG produces a voltage when a temperature gradient (i.e., temperature difference) is established at its sides. Increased inward heat rate at the TEG hot side allows for a much higher temperature gradient across the module and hence increased output voltage generation. This, in turn, improves the power output, which can be noticed from the figures mentioned above. At the start of TEG operation, the temperature difference between the two sides is zero that accordingly will lead to zero output voltage to be generated from the TEG (i.e., zero power output). With the transient time increasing, the temperature difference across the module increases until the steady state operation is achieved. Additionally, it can be observed from figures 4 and 5 that the output voltage and the temperature difference between both sides are almost synchronously achieved stability. Steady state performance is used to summarize and clarify the obtained results.

The effect of input heat rate on the temperature of TEG for both the hot side and cold side is illustrated in figure 12. Figures 12a and 12b show the variation in the temperature of both sides with input heat rates, in case of FC without and with the aid of fins, respectively.

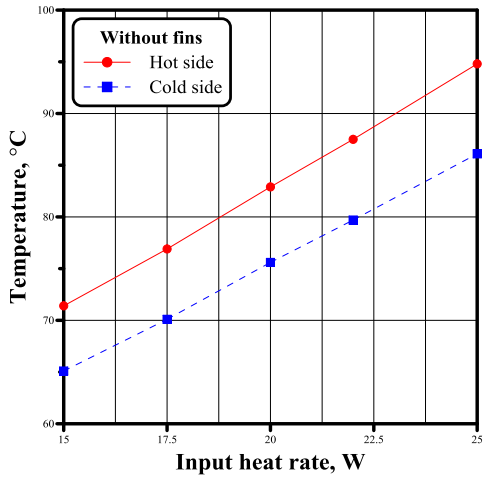

Figure 12a. Variation in the temperature of both sides with input heat rate, without fins.

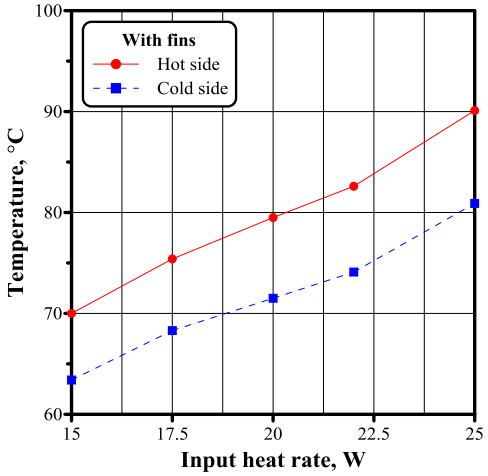

Figure 12b. Variation in the temperature of both sides with input heat rate, with fins.

Figure 12. Effect of input heat rate on the temperature of both sides.

It can be deduced from the figures that the temperature of both sides varies almost linearly with input heat rate. The temperature of the hot and the cold sides are directly proportional to the value of input heat rate. It also noticed that temperature of the cold side is intuitively lower than the temperature of the cold side due to the effect of heat dissipation causing the temperature difference between both sides.

The effect of input heat rate on the output voltage and the corresponding power output of TEG is shown in figure 13. Figures 13a and 13b show the variation in the output voltage and the corresponding power output in case of FC without and with the aid of fins for various input heat rates, respectively. It can be illustrated that the output voltage and consequently the power output is directly proportional to the value of input heat. Increasing the input heat rate will stimulate the temperature difference across the TEG, by increasing the temperature of the hot side that in turn causes a higher output voltage and subsequently enhanced power output. Additionally, it can be noticed that both output voltage and power output follow the same trend for all studied cases. This intuitively returns to the dependency of power output on the output voltage.

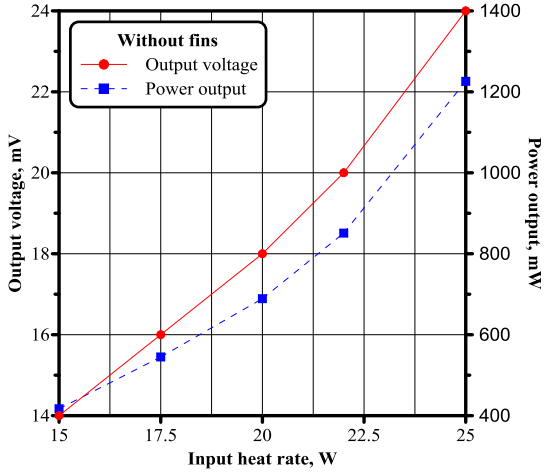

Figure 13a. Variation in the output voltage and power output with input heat rate, without fins.

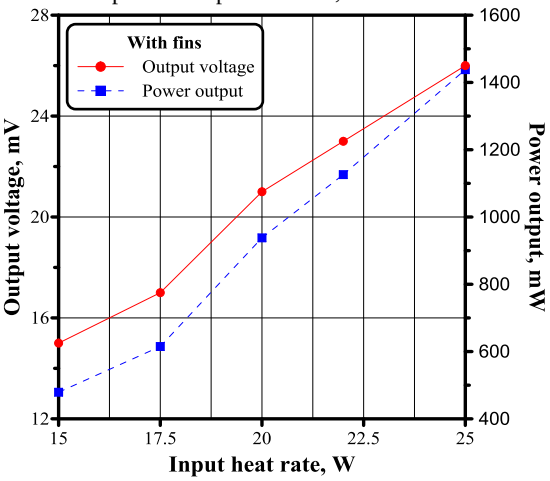

Figure 13b. Variation in the output voltage and power output with input heat rate, with fins.

Figure 13. Effect of input heat rate on the output voltage and power output.

The effect of utilizing fins to aid heat dissipation from the module on the temperature of the TEG hot and cold sides is shown in figure 14. It can be noticed that using fins with the TEG lowers the temperature of both TEG sides by enhancing the rate of heat transfer from the module cold side promoted by increasing the convective heat transfer area subjected to surrounding heat sink. This leads to a higher temperature difference across the TEG with an average increase of 4.8% up to 5.7%.

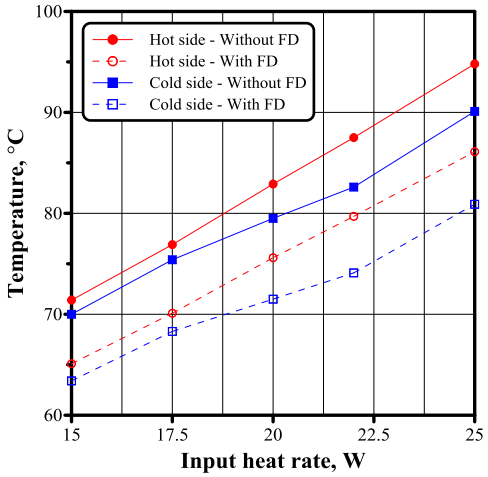

Figure 14. Effect of using fins on the temperature of both sides.

The effect of input heat rate on the output voltage and power output is shown in figure 15. Figures 15a and 15b show the variation in the output voltage and the corresponding power output for various input heat rates, respectively.

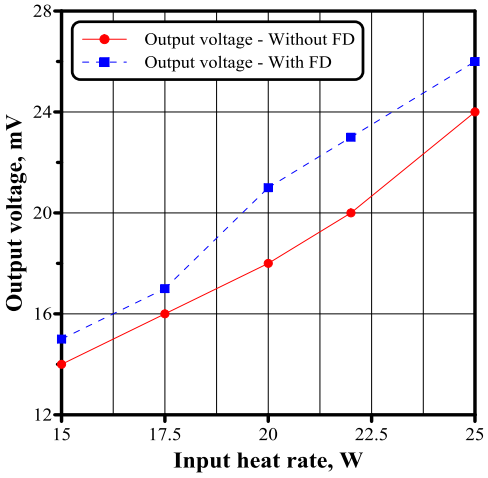

Figure 15a. Variation in the output voltage with input heat rate.

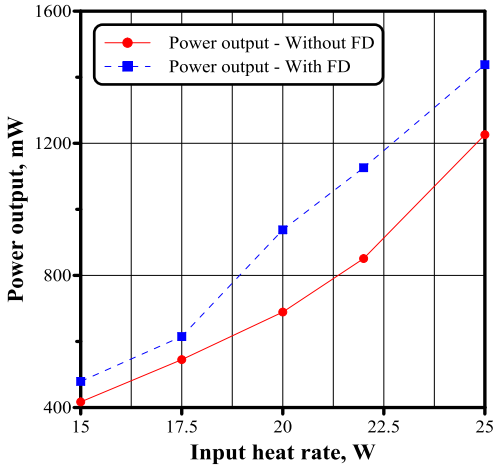

Figure 15b. Variation in the power output with input heat rate.

Figure 15. Effect of using fins on the output voltage and power output.

Since utilizing fins to aid heat transfer from the TEG causes higher temperature difference across the TEG sides it will subsequently improve the output voltage, and in turn, the power output is enhanced with an average increase of 14.9 to 17.3%.

The effect of using fins on the conversion efficiency is shown in figure 16. It can be concluded that the increasing input heat rate will motivate the TEG to generate more output voltage that consequently will increase the power output and promotes, in turn, the acquisition of a higher conversion efficiency. Since the conversion efficiency is defined as the ratio between the power output from the TEG to the rate of heat input, it can be expected that the enhancing effect caused by the utilization of fins on power output for the same input heat rate will consequently improve the conversion efficiency causing an average increase of 14.3% up to 18.4%.

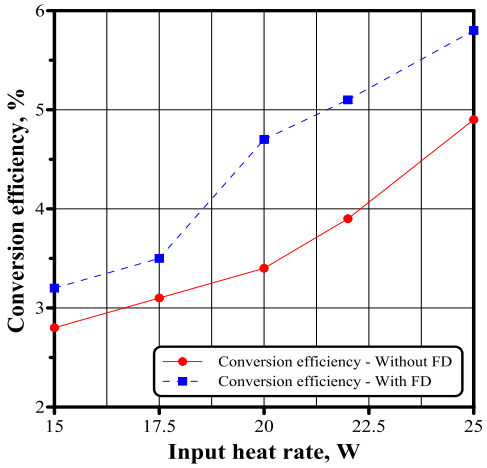

Figure 16. Effect of using fins on the conversion efficiency.

5.3 Comparison between simulation and experimental results

To validate the model and the numerical implementation, data obtained from the experimental study are employed to compare and verify the predicted results obtained from the simulation model. Figure 17 illustrates both experimental and predicted variation in the temperatures of the hot and cold sides with input heat rate. It is shown that an excellent agreement is found between the present experimental and simulation results and the predicted data agrees with the experimental data within 2%. Note that, the model predicted steady state temperature of the sides, slightly higher than the experimental results (i.e. especially the temperature of the cold side with a maximum deviation of 3%), perhaps because the heat loss through the TEG module is not fully considered in the model. If the exact value of the heat loss is impeded in the model, it should be possible to improve the accuracy of predicted data.

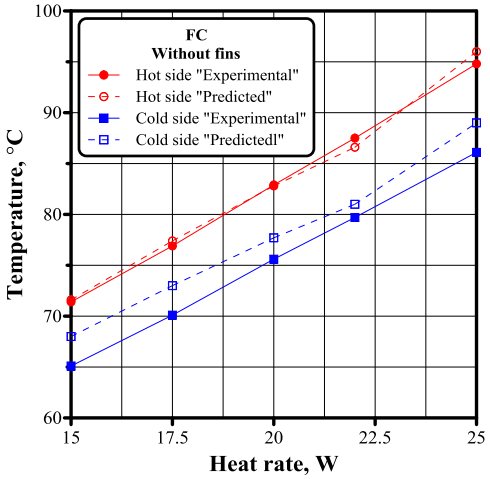

Figure 17. Comparison between both experimental and predicted hot and cold sides temperatures.

The variation in the experimental and predicted output voltage with input heat rate is illustrated in figure 18. It is found that there is a good agreement between the present experimental and simulation results, which verifies the integrity of the modeling procedure. The coincidence between the predicted and experimental values of the output voltage may be attributed to accounting the temperature dependence of thermoelectric material especially Seebeck coefficient and also due to the convergence between experimental and predicted temperature difference.

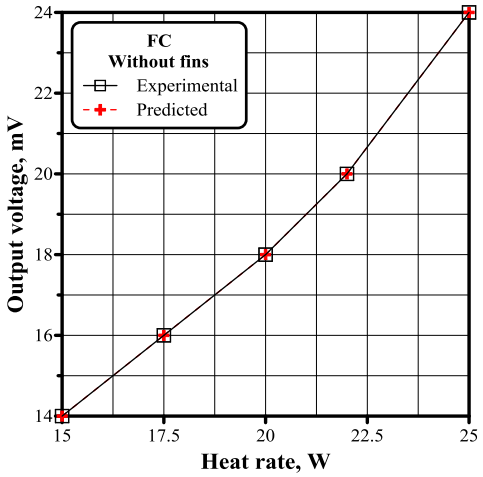

Figure 18. Comparison between both experimental and predicted output voltage.

6. Conclusion

In the present study, a computational and experiential investigation on the transient and steady state performance characteristics of a TEG is carried out.

- A simulation model accounted all the thermoelectric effects besides the dependency of thermoelectric materials on temperature was developed. A computer program based on MATLAB was compiled to solve the model equations.
- The comparison of results between the simulated and experimental data shows a great accuracy and the capability of the developed model to be an efficient simulation tool.
- The effect of varying the input heat rate to the TEG hot side in addition to the effect of utilizing fins to aid the heat dissipation by free air convection from the TEG cold side on the performance is enquired.
- Based on the obtained results of the present study, it can be deduced that increasing the input heat rate causes an increase in both the hot and the cold sides temperatures as well as increasing the temperature difference. Hence, according to the Seebeck effect, the output voltage increases, leading to an increase in the power output and accordingly increases the conversion efficiency.
- In addition, it was observed that utilizing fins to aid heat rejection from the TEG causes an average increase of 14.9% up to 17.3% in power output. This is attributed to the reduction in the temperature of cold side This leads to a higher temperature difference between the module sides, improves the generated output voltage, consequently increases the power output and enhances the conversion efficiency.
- An average increase of 14.9% up to 17.3% in conversion efficiency is achieved by utilizing fins

to aid heat rejection from the TEG. A maximum conversion efficiency achieved was 5.8% in case of 25.0 W input heat rate and utilizing the fins to aid heat dissipation from the module.

References

[1] HoSung L.; "Thermal Design: Heat Sinks, Thermoelectrics, Heat Pipes, Compact Heat Exchangers, and Solar Cells". JOHN WILEY & SONS, INC.; 2011.

[2] Apertet Y., Ouerdane H., Glavatskaya O., Goupil C., Lecoeur P.; "Optimal working conditions for thermoelectric generators with realistic thermal coupling". EPL 2012; 97: 28001 (1-6).

[3] Rezania A., Rosendahl L., Andreasen S.; "Experimental investigation of thermoelectric power generation versus coolant pumping power in a microchannel heat sink". International Communications in Heat and Mass Transfer 2012; 39: 1054-1058.

[4] Admasu B., Luo X., Yao J.; "Effects of temperature non-uniformity over the heat spreader on the outputs of thermoelectric power generation system". Energy Conversion and Management 2013; 76: 533-540.

[5] Bobean C., Valentina P.; "The Study and Modeling of a Thermoelectric Generator Module". The 8th international symposium on advanced topics in electrical engineering 2013.

[6] Jang J., Tsai Y.; "Optimization of thermoelectric generator module spacing and spreader thickness used in a waste heat recovery system". Applied Thermal Engineering 2013; 51: 677-689.

[7] Lesage F., Sempels É., Lalande-Bertrand N.; "A study on heat transfer enhancement using flow channel inserts for thermoelectric power generation". Energy Conversion and Management 2013; 75: 532-541.

[8] Montecucco A., Jonathan Siviter J., Knox A.; "The effect of temperature mismatch on thermoelectric generators electrically connected in series and parallel". Applied Energy 2014; 123: 47-54.

[9] Barma M., Riaz M., Saidur R., Long, B.; "Estimation of thermoelectric power generation by recovering waste heat from Biomass fired thermal oil heater". Energy Conversion and Management 2015; 98: 303-313.

[10] Date A., Date A., Dixon C., Singh R., Akbarzadeh A.; "Theoretical and experimental estimation of limiting input heat flux for thermoelectric power generators with passive cooling". Solar Energy 2015; 111: 201-217.

[11] Barry M., Agbim K., Rao P., Clifford C., Reddy B., Chyu M.; "Geometric optimization of thermoelectric elements for maximum efficiency and power output". Energy 2016; 112: 388-407.

[12] Sarhadi A., Bjørk R., Lindeburg N., Viereck P., Pryds N.; "A thermoelectric power generating heat exchanger: Part II – Numerical modeling and optimization". Energy Conversion and Management 2016; 119: 481-487.

[13] Cao Z., Koukharenko E., Tudor M., Torah R., Beeby S.; "Flexible screen printed thermoelectric generator with enhanced processes and materials". Sensors and Actuators 2016; A238: 196-206.

[14] Chen J., Zuo L., Wu Y., Klein J.; "Modeling, experiments and optimization of an on-pipe thermoelectric generator". Energy Conversion and Management 2016; 122: 298-309.

[15] Du H., Su T., Li H., Li S., Hu M., Liu B., Ma H., Jia X.; "Enhanced low temperature thermoelectric performance and weakly temperature-dependent figure-of-merit values of PbTeePbSe solid solutions". Journal of Alloys and Compounds 2016; 658: 885-890.

[16] Kim T., Negash A., Cho G.; "Waste heat recovery of a diesel engine using a thermoelectric generator equipped with customized thermoelectric modules". Energy Conversion and Management 2016; 124: 280-286.

[17] Shafii M., Shahmohamadi M., Faegh M., Sadrhosseini H.; "Examination of a novel solar still equipped with evacuated tube collectors and thermoelectric modules". Desalination 2016; 382: 21-27.

[18] Shen Z., Wu S., Xiao L., Yin G.; "Theoretical modeling of thermoelectric generator with particular emphasis on the effect of side surface heat transfer". Energy 2016; 95: 367-379.

[19] Wang T., Luan W., Liu T., Tu S., Yan J.; "Performance enhancement of thermoelectric waste heat recovery system by using metal foam inserts". Energy Conversion and Management 2016; 124: 13-19.

[20] Ding L., Meyerheinrich N., Tan L., Rahaoui K., Jain R., Akbarzadeh A.; "Thermoelectric power generation from waste heat of free gas water heater". Energy Procedia 2017; 110: 32-37.

[21] Huang K., Li B., Yan Y., Li Y., Twaha S., Zhu J.; "A comprehensive study on a novel concentric cylindrical thermoelectric power generation system". Applied Thermal Engineering 2017; 117: 501-510.

[22] Li J., Li D., Qin X., Zhang J.; "Enhanced thermoelectric performance of p-type SnSe doped with Zn". Scripta Materialia 2017; 126: 6-10.

[23] Twaha S., Zhu J., Yan Y., Li B., Kuo Huang K.; "Performance analysis of thermoelectric generator using dc-dc converter with incremental conductance based maximum power point tracking". Energy for Sustainable Development 2017; 37: 86-98.

[24] TEG manufacturer datasheet; http://www. europeanthermodynamics.com.